

AE-306

UDC 621.039.548:
621.039.524.46.034

AE-306

Final Report on IFA-10, the first Swedish
Instrumented Fuel Assembly Irradiated in
HBWR, Norway

J-Å. Gyllander



AKTIEBOLAGET ATOMENERGI

STOCKHOLM, SWEDEN 1967

FINAL REPORT ON IFA-10, THE FIRST SWEDISH INSTRUMENTED FUEL ASSEMBLY IRRADIATED IN HBWR, NORWAY

J-Å Gyllander

ABSTRACT

A final report is given on IFA-10, the first Swedish instrumented fuel assembly irradiated in HBWR.

The post-irradiation data are presented and correlated with the irradiation statistics.

No bowing of the bundle was observed, no equi-axed grain growth was discernible, the fission gas release was very small, and the relative dimensional changes in length and diameter were of the order of magnitude 9×10^{-4} .

The hydride content of the can increased from 35 ppm to 65 ppm and, in the contact point of the spacer, to 180 ppm.

Printed and distributed in December 1967.

LIST OF CONTENTS

	<u>Page</u>
1. Introduction	3
2. Objectives of IFA-10	3
3. Design and description of IFA-10	3
3.1 Assembly design	3
3.2 Instrumentation	3
4. Irradiation conditions	4
4.1 Irradiation history	4
4.2 Heat ratings	4
5. Post-irradiation examination	4
5.1 Visual inspection	4
5.2 Dimensional measurement	5
5.3 Crud measurement	5
5.4 Fission gas release	5
5.5 γ -scanning	6
5.6 Ceramography	6
5.7 Hydrogen pick-up	6
6. Discussion of the results	6
6.1 Heat ratings and UO_2 temperature effects	6
6.1.1 Thermal conductivity	6
6.1.2 Fission gas release	7
6.1.3 Grain growth	8
6.2 Dimensional changes	8
6.2.1 Assemblies	8
6.2.2 Individual rods	8
6.3 Spacer design	8
6.3.1 Stability	8
6.3.2 Fretting	8
6.3.3 Hydrogen pick-up	8
6.3.4 Crud deposition	8

	<u>Page</u>
7. Conclusions for the actual experiment	9
7.1 Feasibility of long fuel stringers	9
7.2 Deformation behaviour of a six-rod element	9
7.3 The effect of the spacers	9
7.4 Thermal conductivity of UO_2	9
8. References	10
9. List of computer programs used	12
10. List of figures	13

Tables

Figures

1. INTRODUCTION

During the period January 1964 to December 1966 AB Atomenergi, Sweden has extended its collaboration in the OECD Halden Project to a series of experimental fuel assemblies in the Halden Boiling Water Reactor, HBWR. The first Swedish test fuel assembly was designated IFA-10 and the final report on this experiment is given below.

2. OBJECTIVES OF IFA-10

The main purposes of this irradiation experiment were the following:

- i) to study the possibility of using long fuel stringers in element design,
- ii) to study the form of deformation, if any, arising in a six-rod element irradiated in conditions as close to those of the Marviken reactor as possible,
- iii) to test the effectivity of the strip spacer design with respect to avoiding fretting of the rods,
- iv) to test the corrosion rate due to the spacer strip,
- v) to measure the heat conductivity of the actual oxide fuel.

See also ref. [1, 2, 3 and 15].

3. DESIGN AND DESCRIPTION OF IFA-10

3.1 Assembly design

The fuel bundle consisted of six rods UO_2 canned in Zr-2 and arranged with one central and five equally spaced circumferential rods. The active length of each of the rods was 1714 mm and they were separated by three strip spacers along the length. The pellet diameter was 12.47 mm and the shroud tube had an inner diameter of 71 mm.

3.2 Instrumentation

The assembly was equipped with instruments to measure power, flow, exit steam quality, central oxide temperature and the coolant temperature. These signals were registered continuously during the irradiation. The total UO_2 -stack movement after irradiation was meas-

ured in five of the rods. The integrated thermal neutron dose was measured by means of internal cobalt monitors along the circumference of some of the pellets. See also ref. [1,4,9,15 and 19] and fig. 1-5.

4. IRRADIATION CONDITIONS

4.1 Irradiation history

Fig. 16 gives the channel power as a function of in-core time. It is obvious that the evaluation of the data must be divided into two different power-steps:

- I High-power, 340 kW
- II Medium-power, 275 kW

In tables 1, 3, 6, 7 and 8 this division has been made.

4.2 Heat ratings

The heat ratings have been calculated by an axial form factor of 1.27. The radial form factors have been calculated from the burn-up values.

In fig. 17 the relationship between channel power, linear heat output, heat conductivity integral, heat surface flux on the canning and specific power is given for the highest and lowest heat rated rods D and C respectively. The dashed line in the middle corresponds to a hypothetical rod with FRAD = 1.

The computer programs 1, 2, 3, 6, 7 and 8 have been used for the various calculations.

5. POST-IRRADIATION EXAMINATION

5.1 Visual inspection

The visual inspection of the fuel assembly did not reveal any special effects. The only thing was a thin layer of crud which can be seen in fig. 14-15. The layer had a typical streaming pattern behind the spacers and it was very easily removed. Under section 6.3 the crud measurement will be discussed.

After dismantling one could observe small fretting marks on the can surface caused by the spacers (see fig. 6 and 7).

5.2 Dimensional measurement (by B Winqvist)

The dimensional measurements have included determination of radial and tangential rod profiles, distance between adjacent rods in an assembled bundle, and measurements of diameter and profile of de-mounted central rods.

In connection with the measurement of tangential profiles, the diameters of the outer rods have been determined.

The measurements have been carried out in our measuring rig Goliath. Zeroing of the rig measuring head has been carried out by mounting together gauge blocks until they nominally formed the distance concerned.

The following gauge blocks have been used (fig. 18)

Determination of radial profile (by scanning along the 0° generator).
Gauge block, $\emptyset 57.00 \pm 0.01$ mm.

Determination of tangential profile and rod diameter (by scanning along the 270° and $270-90^{\circ}$ generators). Gauge block, $\emptyset 14.00 \pm 0.001$ mm.

Determination of separation between adjacent rods (by scanning along the 36° and 324° generators). Gauge block $\emptyset 39.00 \pm 0.01$ mm.

The results are summarized in table 4, where the UO_2 stack movement relative to the can is also given. See also ref. [4, 6, 8, 9 and 16].

5.3 Crud measurement

As mentioned in paragraph 5.1 the crud was very easily removed. Six crud samples were taken and analyzed. The positions of the samples and the analysis values are given in tables 9-11. See also ref. [22].

5.4 Fission gas release

The fission gas release was measured for five rods. The gas was analyzed by γ -spectrometry and mass-spectrometry and the release values were calculated by the computer program FARMA. The values are given in table 12.

5.5 γ -scanning

Longitudinal γ -scanning was performed for all the six rods. The energy used for the γ -scanning was 0.75 MeV (Zr-Nb) and the curves are reproduced in fig. 19-24.

5.6 Ceramography

According to the γ -scanning the highest heat-rated pellets were taken for ceramography. The results are shown in fig. 10-13, fig. 10 from rod A, fig. 11-13 from rod D, the same area at various magnifications.

5.7 Hydrogen pick-up

From rod E six samples were taken for hydride measurements. The reference mark is shown in fig. 7, and fig. 8 and 9 show the resulting can after the samples were taken. The results are given in detail in fig. 25 and are summarized in table 5.

6. DISCUSSION OF THE RESULTS

6.1 Heat ratings and UO_2 temperature effects

6.1.1 Thermal conductivity

With only one oxide thermocouple it is not possible to determine the thermal conductivity of UO_2 for the following reasons

- a) the heat transfer coefficient of the clearance between canning and UO_2 has a great influence,
- b) the assumed thermal neutron distribution and hence the heat generation distribution cannot be checked.

In addition to these points rod A, which was equipped with the thermocouple, had an enrichment of 2.5 w/o U-235 in the lower part of the rod (835.6 mm) and 2.8 w/o U-235 in the upper part of the rod (878.4 mm). The other five rods had an enrichment of 2.8 w/o U-235 along the whole length. Hence, the heat rating figure for the thermocouple rod, in the plane where the thermocouple was positioned, are not given in table 3, but the temperature distribution in table 6 is cal-

culated according to a linear heat output of 323, 400, and 409 W/cm respectively, corresponding to a heat conductivity integral of 24.8, 30.7, and 31.4 W/cm respectively.

In ref. [11] the integral values given in table IV are not corrected either for the radial form factors, the internal form factors, or the different enrichments. The temperature figures corresponding to the element power Q_A of approximately 340 kW (6407122320, 6407160900 and 6407211410) which are 1395, 1415, and 1420 °C respectively, are about 20 °C higher than those calculated with the recommended value of heat transfer coefficient given in ref. [14] ($a = 1.0 \text{ W/cm}^2 \cdot \text{°C}$ for an assembly clearance of 0.016 cm) and with the thermal conductivity value recommended by AB Atomenergi, ref. [24,25]. The agreement is not so good at lower heat ratings - probably owing to an improper choice of a .

6.1.2 Fission gas release

The values given in table 12 are very small. The reason for this is very clearly understood by comparing fig. 16, 17, tables 1, 3, 7 and 8. The values in table 12, which are computed by the program FARMA, is fractional gas release (f. g. r.) in percent. Fig. 16 shows that the higher element power of 340 kW is only achieved at the beginning of the irradiation and table 1 shows that this power level only corresponds to 30.4 % of the total burn-up. So, in fact, in order to calculate the fission gas release for the 340 kW period only, one must multiply by the factor $\frac{100}{30.4}$ which gives a f. g. r. of 0.07 %.

The explanation for this very low figure is given in tables 7 and 8. Even at the highest heat-rated rod D, the volume of UO_2 which is over 1600 °C is only 1.6 % of the total volume. The remarkably low f. g. r. values are therefore in full accord with experience. If we assume no fission gas release below 1600 °C the result will be

$$\text{f. g. r.} \leq \frac{100}{30.4} \cdot \frac{100}{1.6} \cdot 0.02 \% = 6 \%$$

over 1600 °C.

6.1.3 Grain growth

The same discussion as in point 6.1.2 gives the explanation for the absence of grain growth.

6.2 Dimensional changes

6.2.1 Assemblies

The overall stability of the bundle was surprisingly good. No bowing was detectable.

6.2.2 Individual rods

The results are summarized in table 4. The dimensional changes were small.

6.3 Spacer design

6.3.1 Stability

As already mentioned in paragraph 6.2.1, the stability of the bundle was good.

6.3.2 Fretting

As shown in fig. 6 and 7 the fretting marks were small. The photographs show the worst fretting mark of the whole bundle.

6.3.3 Hydrogen pick-up

In table 5 and fig. 25 the hydride content values are given. The measurements show a pronounced hydrogen pick-up in the vicinity of the spacer.

6.3.4 Crud deposition

The visual examination revealed a streaming pattern behind the spacer in the form of a very thin crud layer. The thickness of the crud does not seem to affect the heat transfer appreciably.

7. CONCLUSIONS FOR THE ACTUAL EXPERIMENT

7.1 Feasibility of long fuel stringers

Long fuel stringers are feasible.

7.2 Deformation behaviour of a six-rod element

No deformation of the bundle was detected.

7.3 The effect of the spacers

The chosen spacer design was good with respect to stability and fretting, but had a drawback in view of hydrogen pick-up.

7.4 Thermal conductivity of UO₂

The experiment confirmed the out-of-pile data up to 1400 °C with a heat transfer coefficient of 1.0 W/cm² · °C.

8. REFERENCES

1. DJURLE S,
1963. AB Atomenergi, Sweden. (Internal report RMA-403.)
2. BJÖRKLUND K,
1964. AB Atomenergi, Sweden. (Internal report TPM-RMB-495.)
3. DJURLE S,
1964. AB Atomenergi, Sweden. (Internal report RM-203.)
4. BJÖRKLUND K,
1964. AB Atomenergi, Sweden. (Internal report TPM-RMB-351
rev. 1.)
5. GOODE G,
1964. AB Atomenergi, Sweden. (Internal report TPM-RKS-161.)
6. BJÖRZÉN H,
1964. AB Atomenergi, Sweden. (Internal report AP-RMB-891.1-1.)
7. KRELL Å,
1964. AB Atomenergi, Sweden. (Internal report TPM-RFA-578.)
8. ERIKSSON E,
1964. AB Atomenergi, Sweden. (Internal report AP-RMB-891.2-1.)
9. BJÖRKLUND K,
1964. AB Atomenergi, Sweden. (Internal report TPM-RMB-550.)
10. JONASSON G,
1964. AB Atomenergi, Sweden. (Internal report TPM-RKS-169.)
11. ROLSTAD E,
1964. Institutt for Atomenergi, Norway. (Internal report EPB-305.)
12. HALLSTENSSON L,
1964. AB Atomenergi, Sweden. (Internal report TPM-RMB-596.)
13. FORSBERG L, GOODE G,
1964. AB Atomenergi, Sweden. (Internal report STK-178.)
14. GYLLANDER J-Å,
1964. AB Atomenergi, Sweden. (Internal report TPM-RMA-541.)
15. ASPHAUG K,
1964. Institutt for Atomenergi, Norway. (Internal report DP-305.)
16. FILIPSSON B,
1964. AB Atomenergi, Sweden. (Internal report AP-RMB-891.1-2.)
17. KRELL Å,
1964. AB Atomenergi, Sweden. (Internal report TPM-RFA-559.)

18. FREDRIKSSON F,
1964. AB Atomenergi, Sweden. (Internal report TPM-RFR-292.)
19. SVENSSON S,
1964. AB Atomenergi, Sweden. (Internal report RFA-598.)
20. GYLLANDER J-Å,
1965. AB Atomenergi, Sweden. (Internal report TPM-RMA-579.)
21. GYLLANDER J-Å,
1965. AB Atomenergi, Sweden. (Internal report TPM-RMA-596.)
22. EDWALL B, LUNDQVIST R,
1965. AB Atomenergi, Sweden. (Internal report AP-RKK-98.)
23. GYLLANDER J-Å,
1967. AB Atomenergi, Sweden. (Internal report TPM-RMA-710.)
24. VOGT J, GRANDELL L, RUNFORS U,
1964. AB Atomenergi, Sweden. (Internal report RMB-527.)
25. RUNFORS U,
1966. AB Atomenergi, Sweden. (Internal report RMB-1089.)

9. LIST OF COMPUTER PROGRAMS USED

1.	INDO, integrated neutron dose and burn-up program	S Svensson
2.	SLIRMA, loop program in general	J-Å Gyllander
3.	FIRMA, neutron flux from Co-monitors	J-Å Gyllander
4.	FARMA, fission gas release	B Danielsson
5.	GORMA, dimensional changes	J-Å Gyllander
6.	BURMA, chemical burn-up measurement	J-Å Gyllander
7.	TERMA, temperature distribution	J-Å Gyllander
8.	VORMA, volume distribution	J-Å Gyllander
9.	STARMA, statistics program	J-Å Gyllander
10.	KORRMA, correlation program	J-Å Gyllander

Program 1 is described in detail in ref. [19] and programs 2-10 are described in ref. [23].

10. LIST OF FIGURES

1. Top plug with gauge plug
2. Spacer
3. Upper end of the bundle
4. Upper end of the bundle
5. Lower end of the bundle
6. Fretting mark on spacer
7. Fretting mark on rod E
8. Position of samples for hydride measurement
9. Position of samples for hydride measurement
10. Transversal cut rod A in axial maximum
11. Transversal cut rod D in axial maximum
12. Detail of fig. 11, 14 x magnification
13. Detail of fig. 11, 500 x magnification
14. Fuel bundle, bottom, after irradiation
15. Fuel bundle, top, after irradiation
16. Irradiation history
17. Diagram over certain heat data as a function of channel power
18. Goliath gauges
- 19-
24. γ -scanning curves
25. The samples for the hydride measurement

TABLE 1

Irradiation statistics

Element Power P kW	Time		Burn-up	
	Days	%	MWd	%
P = 0	43.2	19.5	-	-
0 < P < 100	16.7	7.6	0.9	2.1
100 ≤ P < 200	9.6	4.3	1.5	3.3
200 ≤ P < 300	110.7	50.1	29.1	64.2
300 ≤ P	40.8	18.5	13.8	30.4
Total	221.0	100.0	45.3	100.0

TABLE 2

Burn-up by means of chemical-massspectrometric analysis

Rod	FIMA Max	FIMA Average	MWd/t UO ₂ Average	Ton UO ₂	MWd
A	$5.50 \cdot 10^{-3}$	$4.08 \cdot 10^{-3}$	3420	$2.164 \cdot 10^{-3}$	7.40
B	5.16	4.06	3400	2.170	7.38
C	4.52	3.56	2980	2.171	6.47
D	5.55	4.36	3660	2.174	7.96
E	5.43	4.27	3580	2.174	7.78
F	4.74	3.73	3130	2.173	6.80
Total					43.79

TABLE 3

Radial form factors, FRAD, linear heat output Q(275) and Q(340), average at total element power of 275 resp. 340 kW

Rod	FRAD	Q(275) W/cm	Q(340) W/cm
A	1.068	-	-
B	1.003	271	335
C	0.877	237	293
D	1.077	291	360
E	1.054	285	352
F	0.920	248	307

TABLE 4

Dimensional changes, ridge heights and UO₂ stack movement

Rod	FRAD	Length °/oo	Diameter		Ridge height µm	UO ₂ stack movement °/oo
			Max µm	Min µm		
A	1.068	-	- 15	+ 5	5	1.5
B	1.003	+ .79	+ 7	+ 19	5	1.2
C	0.877	+ .78	+ 9	+ 11	10	1.1
D	1.077	+ .87	+ 6	+ 11	5	.9
E	1.054	+ .94	+ 18	+ 13	3	1.4
F	0.912	+ .76	- 2	+ 3	13	.4

TABLE 5

Hydride formation

Rod		E
Spacer No. (from bottom)		3
Height over bottom	(cm)	88
Outside can temperature	(°C)	245
Hydride content of the can	(ppm)	
just below spacer		65
contact point		180
Reference (non-irradiated)		35

TABLE 6

Temperature distribution (°C), rod A (thermocouple)

Radius (mm)	Element power (kW)		
	275	340	348
0.00	1082	1379	1416
0.50	1077	1371	1407
1.00	1060	1347	1383
1.50	1033	1308	1343
2.00	995	1255	1287
2.50	947	1187	1217
3.00	891	1107	1134
3.50	826	1017	1040
4.00	755	917	937
4.50	679	811	827
5.00	598	700	713
5.50	515	589	597
6.00	431	477	483
6.23	391	426	430

TABLE 7

Temperature distribution ($^{\circ}\text{C}$), rod D

Radius (mm)	Element power (kW)	
	275	340
0.00	1255	1618
0.50	1248	1609
1.00	1227	1580
1.50	1193	1532
2.00	1146	1466
2.50	1087	1383
3.00	1017	1284
3.50	937	1171
4.00	850	1048
4.50	756	917
5.00	658	781
5.50	558	646
6.00	459	513
6.23	412	452

TABLE 8

Integrated volumes for rod D

Temperature interval	275 kW		340 kW	
	cm ³	%	cm ³	%
300 - 500	60.0	28.7	37.0	17.7
500 - 600	40.5	19.4	32.8	15.7
600 - 700	32.0	15.3	29.8	14.3
700 - 800	24.5	11.7	24.5	11.7
800 - 900	18.8	9.0	19.8	9.5
900 - 1000	14.4	6.9	16.3	7.8
1000 - 1100	10.5	5.0	13.4	6.4
1100 - 1200	6.8	3.3	11.0	5.3
1200 - 1300	1.9	8.9	9.0	4.3
1300 - 1400	0.0	0.0	7.1	3.4
1400 - 1500			5.3	2.5
1500 - 1600			3.2	1.5
1600 - 1700			0.2	0.1
1700 - 1800			0.0	0.0

Crud measurements

The positions of the samples are given in the sketch below.

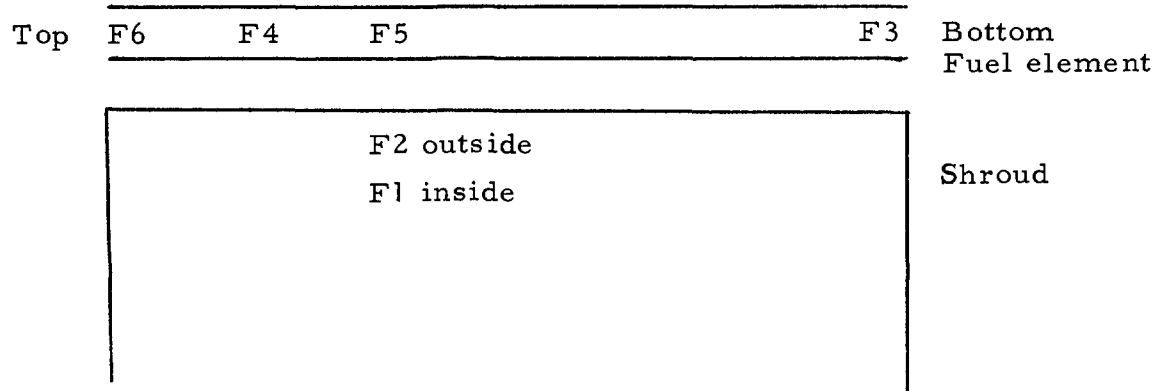


TABLE 9

Crud deposition ($\mu\text{g}/\text{cm}^2$)

	Fe	Ni	Cr	Zr
F1	32	8	5	> 2
F2	4	< 2	< 2	> 2
F3	8	< 2	< 2	15
F4	8	< 2	< 2	15
F5	8	< 2	< 2	> 2
F6	12	< 2	< 2	> 2

TABLE 10

The crud activities 22.9.65 (dps/cm²)

	Co-58	Co-60	Zr-95	Fe-59	Cr-51	Mn-54
F1	$8.5 \cdot 10^2$	$1.2 \cdot 10^3$	$3.8 \cdot 10^3$	$2.3 \cdot 10^2$	$2.4 \cdot 10^3$	$9.7 \cdot 10^1$
F2	$3.4 \cdot 10^2$	$2.2 \cdot 10^3$	$1.1 \cdot 10^3$	$3.5 \cdot 10^2$	$1.0 \cdot 10^3$	$1.80 \cdot 10^2$
F3	$5.6 \cdot 10^2$	$1.0 \cdot 10^3$	$1.5 \cdot 10^3$	$1.8 \cdot 10^2$	$1.2 \cdot 10^3$	$6.9 \cdot 10^1$
F4	$7.5 \cdot 10^2$	$2.0 \cdot 10^3$	$2.0 \cdot 10^3$	$2.0 \cdot 10^2$	$2.2 \cdot 10^3$	$1.90 \cdot 10^2$
F5	$5.2 \cdot 10^2$	$2.0 \cdot 10^2$	$1.4 \cdot 10^3$	$1.2 \cdot 10^2$	$7.6 \cdot 10^2$	$1.30 \cdot 10^2$
F6	$4.7 \cdot 10^3$	$7.3 \cdot 10^2$	$1.8 \cdot 10^4$	$2.5 \cdot 10^3$	$6.4 \cdot 10^4$	$1.7 \cdot 10^3$

TABLE 11

Specific activities (dps/mg Fe)

	Co-58	Co-60	Zr-95	Fe-59	Cr-51	Mn-54
F6	$3.92 \cdot 10^5$	$6.08 \cdot 10^4$	$1.5 \cdot 10^6$	$2.08 \cdot 10^5$	$5.33 \cdot 10^6$	$1.42 \cdot 10^5$
F4	$9.37 \cdot 10^4$	$2.50 \cdot 10^5$	$2.50 \cdot 10^5$	$2.50 \cdot 10^4$	$2.75 \cdot 10^5$	$2.37 \cdot 10^4$
F5	$6.50 \cdot 10^4$	$2.50 \cdot 10^4$	$1.75 \cdot 10^5$	$1.50 \cdot 10^4$	$9.5 \cdot 10^4$	$1.63 \cdot 10^4$
F3	$7.0 \cdot 10^4$	$1.25 \cdot 10^5$	$1.88 \cdot 10^5$	$2.25 \cdot 10^4$	$1.5 \cdot 10^5$	$8.63 \cdot 10^3$
F1	$2.66 \cdot 10^4$	$3.75 \cdot 10^4$	$1.19 \cdot 10^5$	$7.19 \cdot 10^3$	$7.5 \cdot 10^4$	$3.03 \cdot 10^3$
F2	$8.5 \cdot 10^4$	$5.5 \cdot 10^5$	$2.75 \cdot 10^5$	$8.75 \cdot 10^4$	$2.5 \cdot 10^5$	$4.5 \cdot 10^4$

TABLE 12

Fission gas release (%)

Rod	A	B	C	D	E	F
Kr	-	0.02	0.03	0.02	0.02	0.02
Xe	-	0.02	0.03	0.03	0.02	0.02

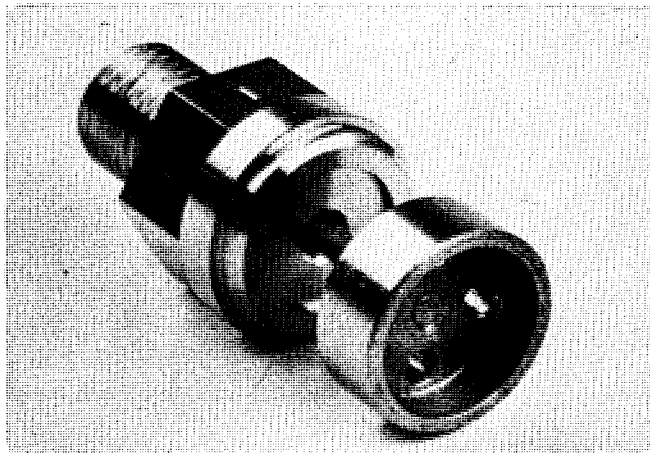


Fig. 1 Top plug with gauge plug

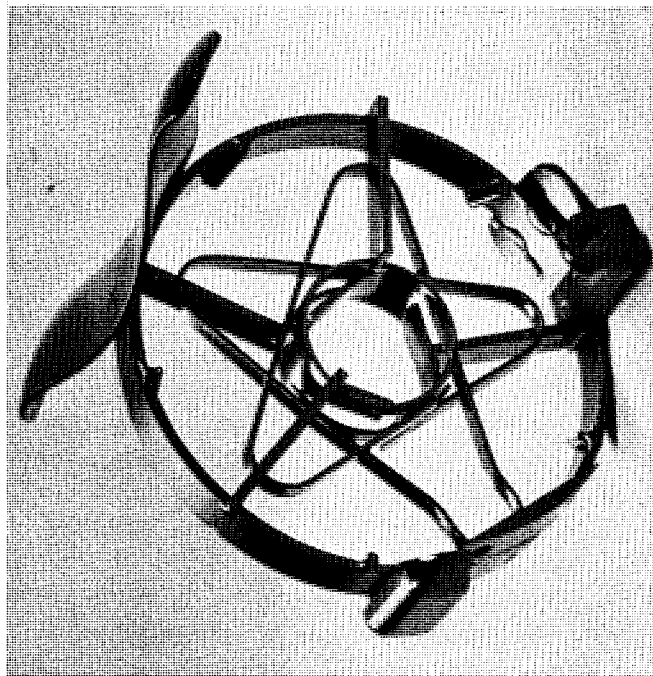


Fig. 2 Spacer

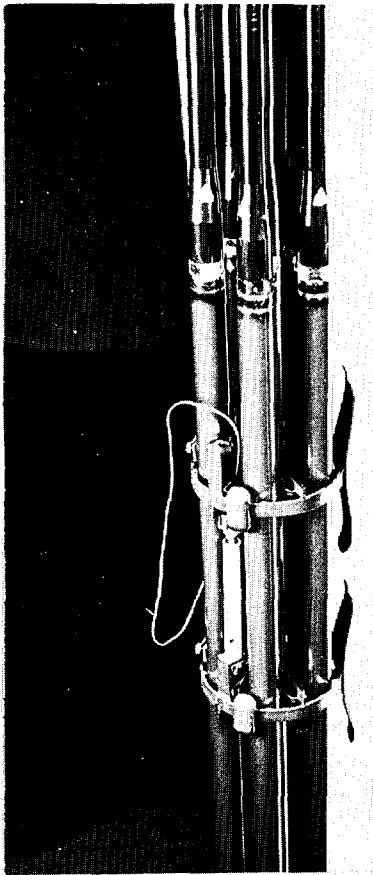


Fig. 3 Upper end of the bundle

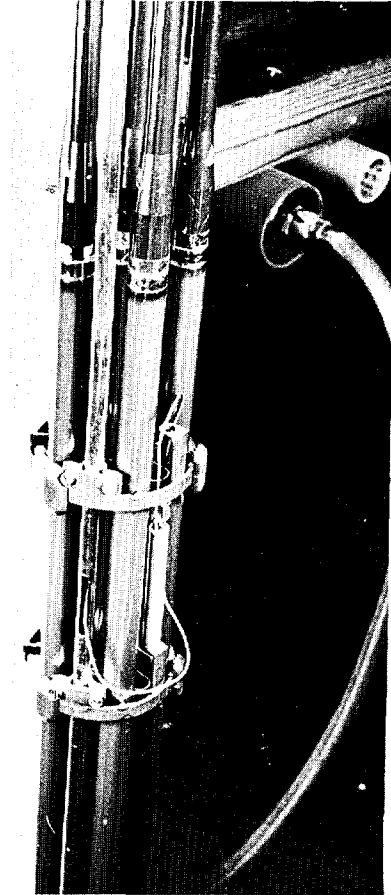


Fig. 4 Upper end of the bundle

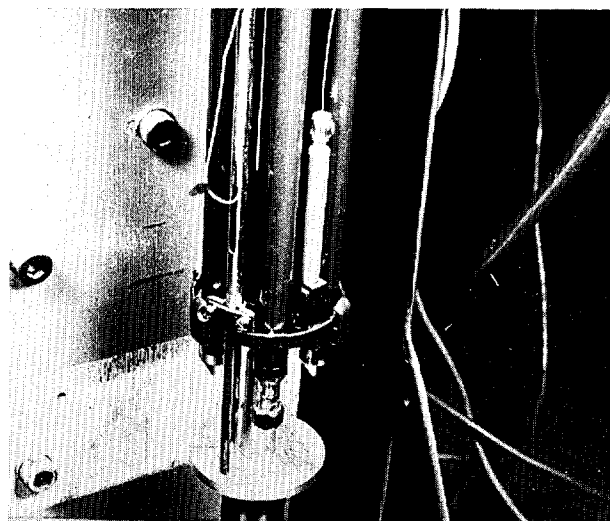


Fig. 5 Lower end of the bundle

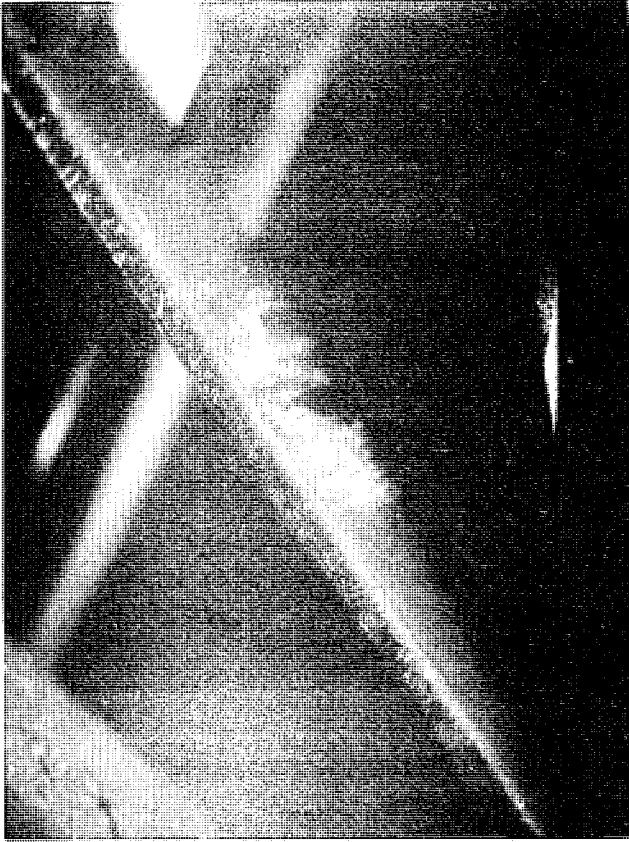


Fig. 6

4.5x



Fig. 7

4.5x

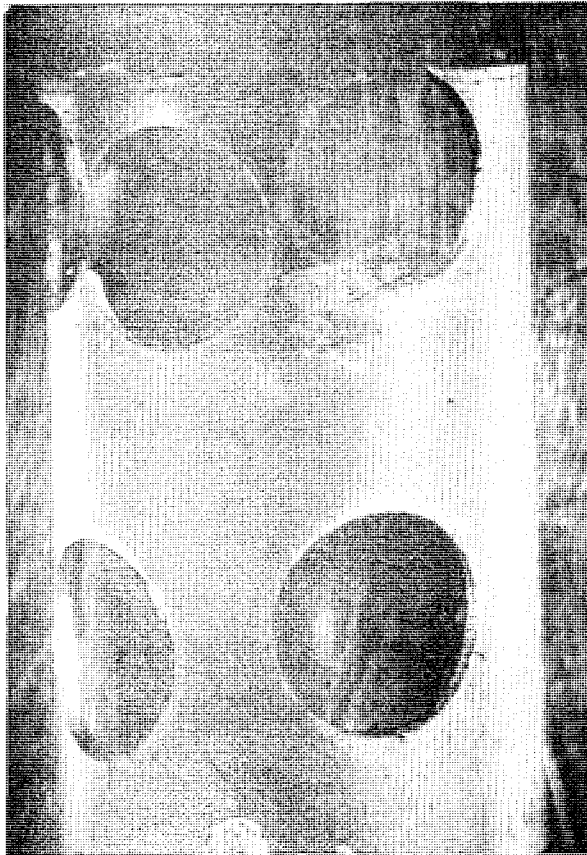


Fig. 8

4.5x

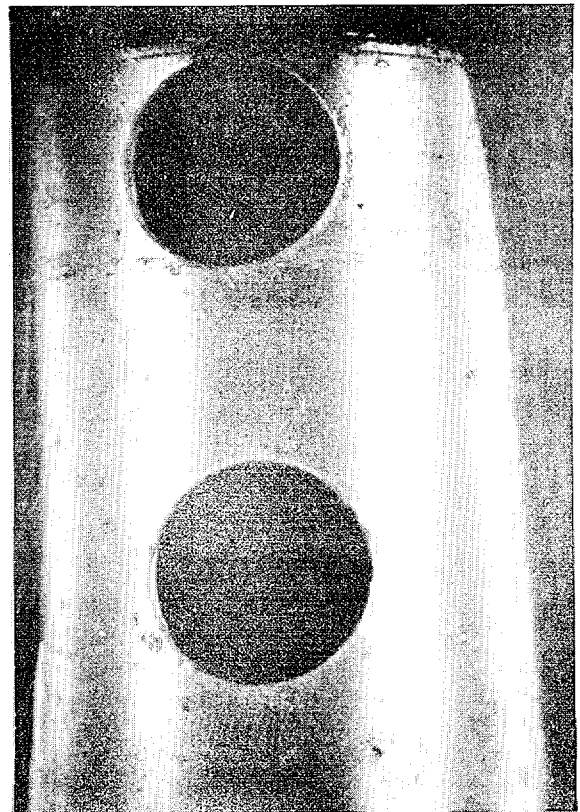


Fig. 9

4.5x

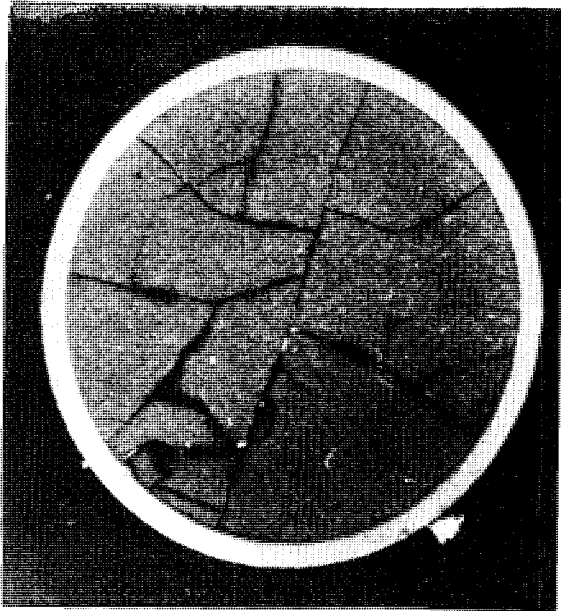


Fig. 10

4.5x

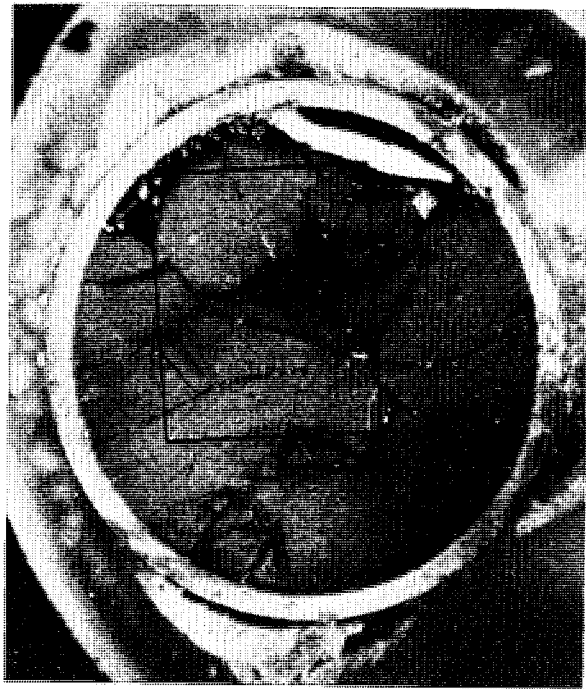


Fig. 11

4.5x

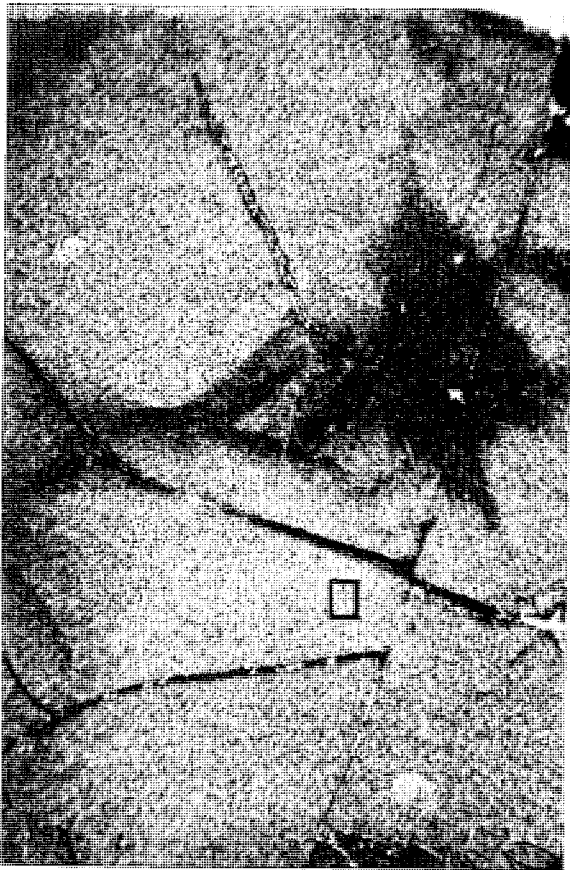


Fig. 12

14x

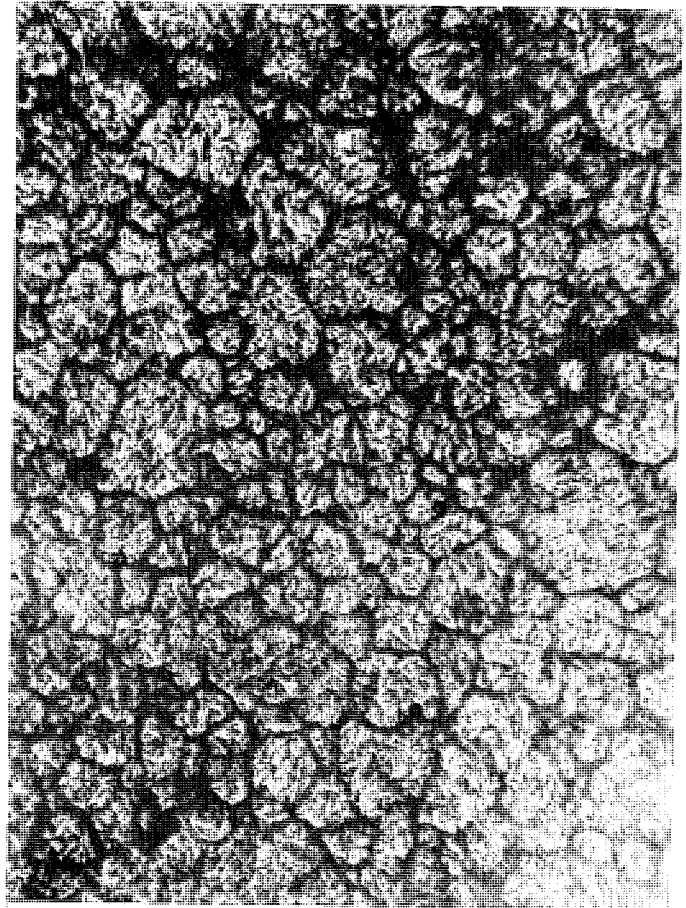


Fig. 13

500x

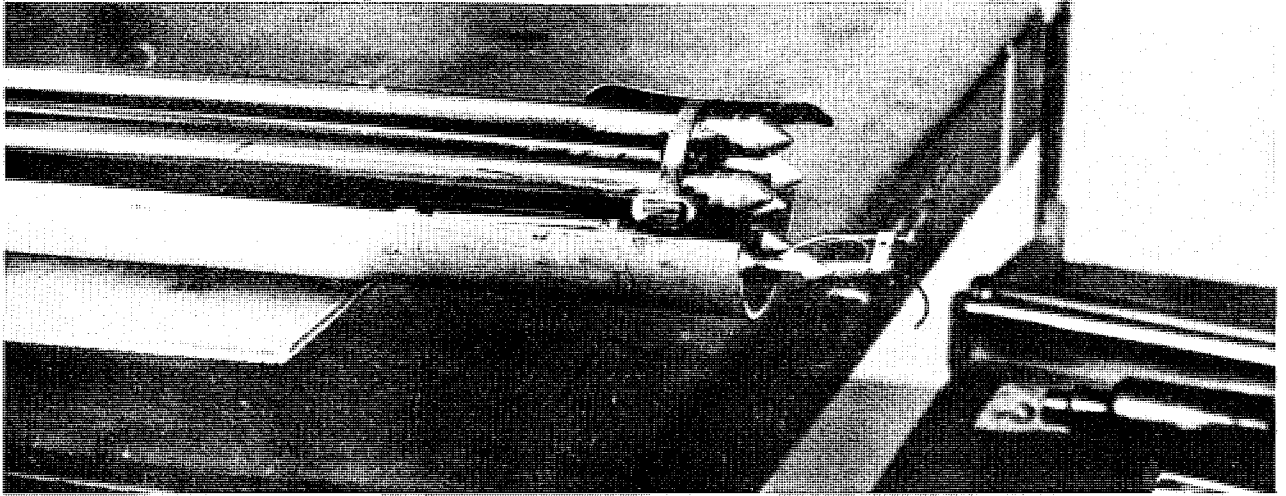


Fig. 14 Through cell window

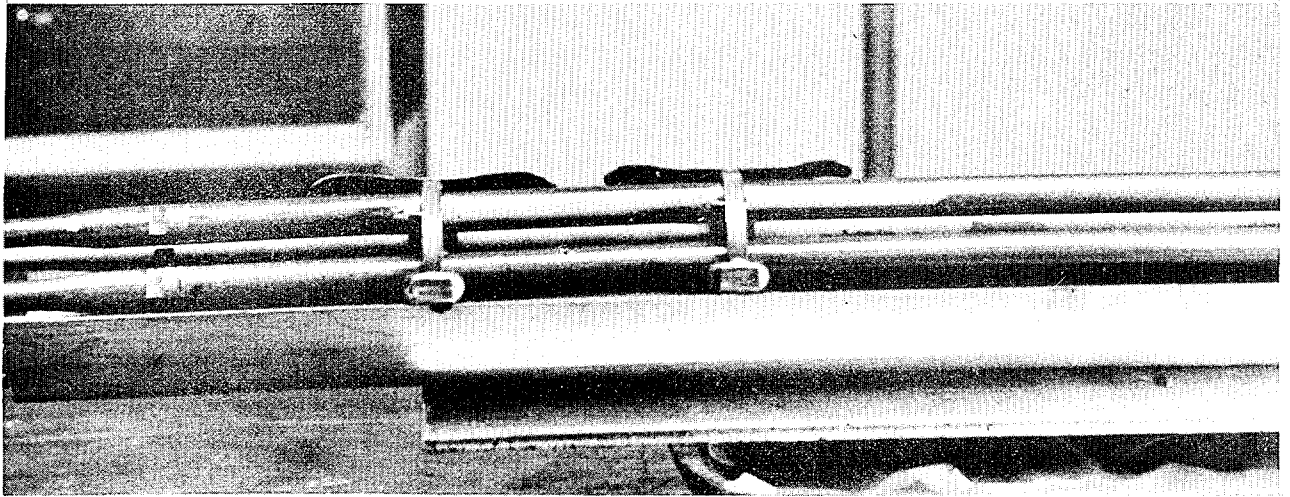
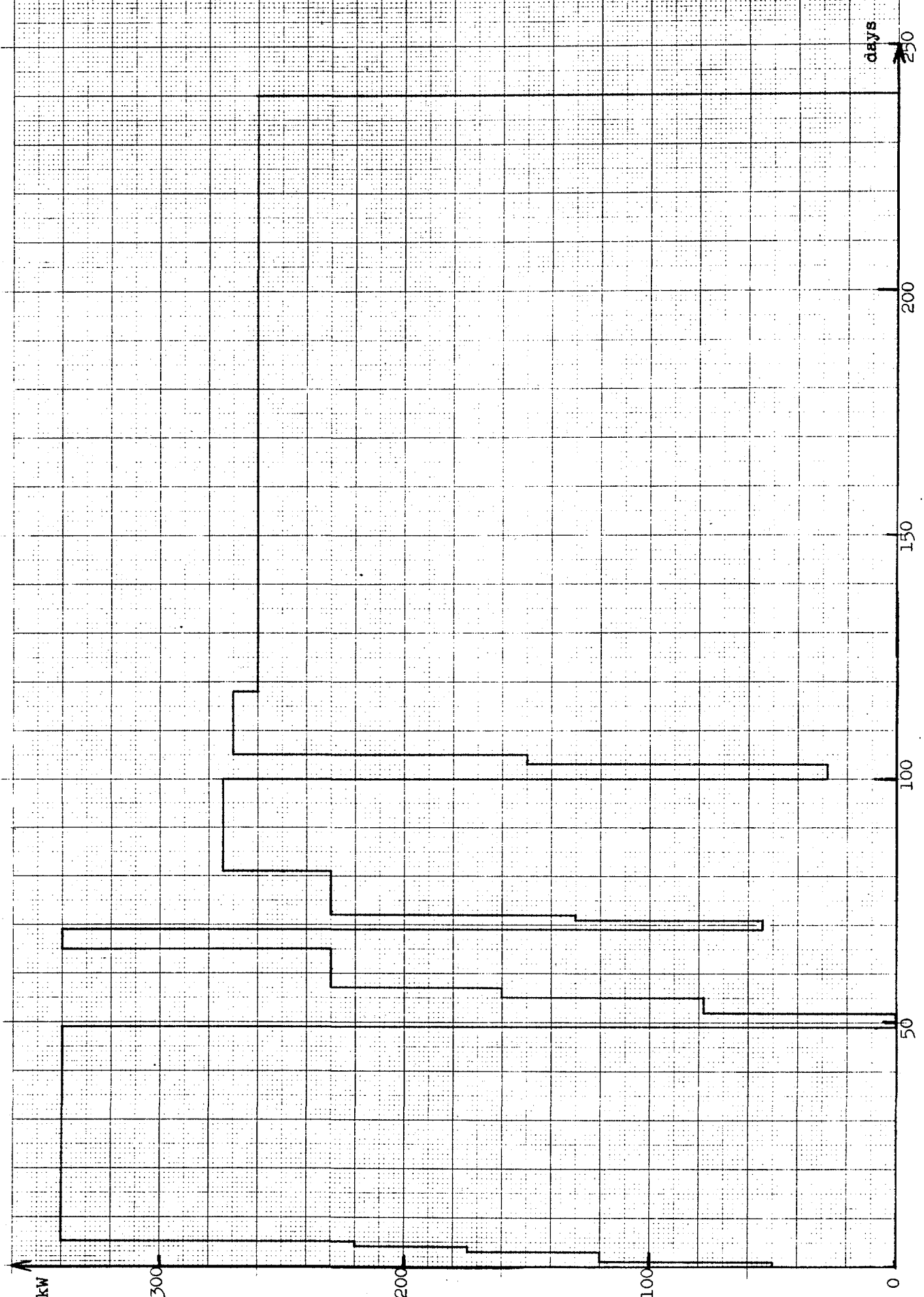


Fig. 15 Through cell window

Irradiation history

Channel power in kW as a function of in-core time

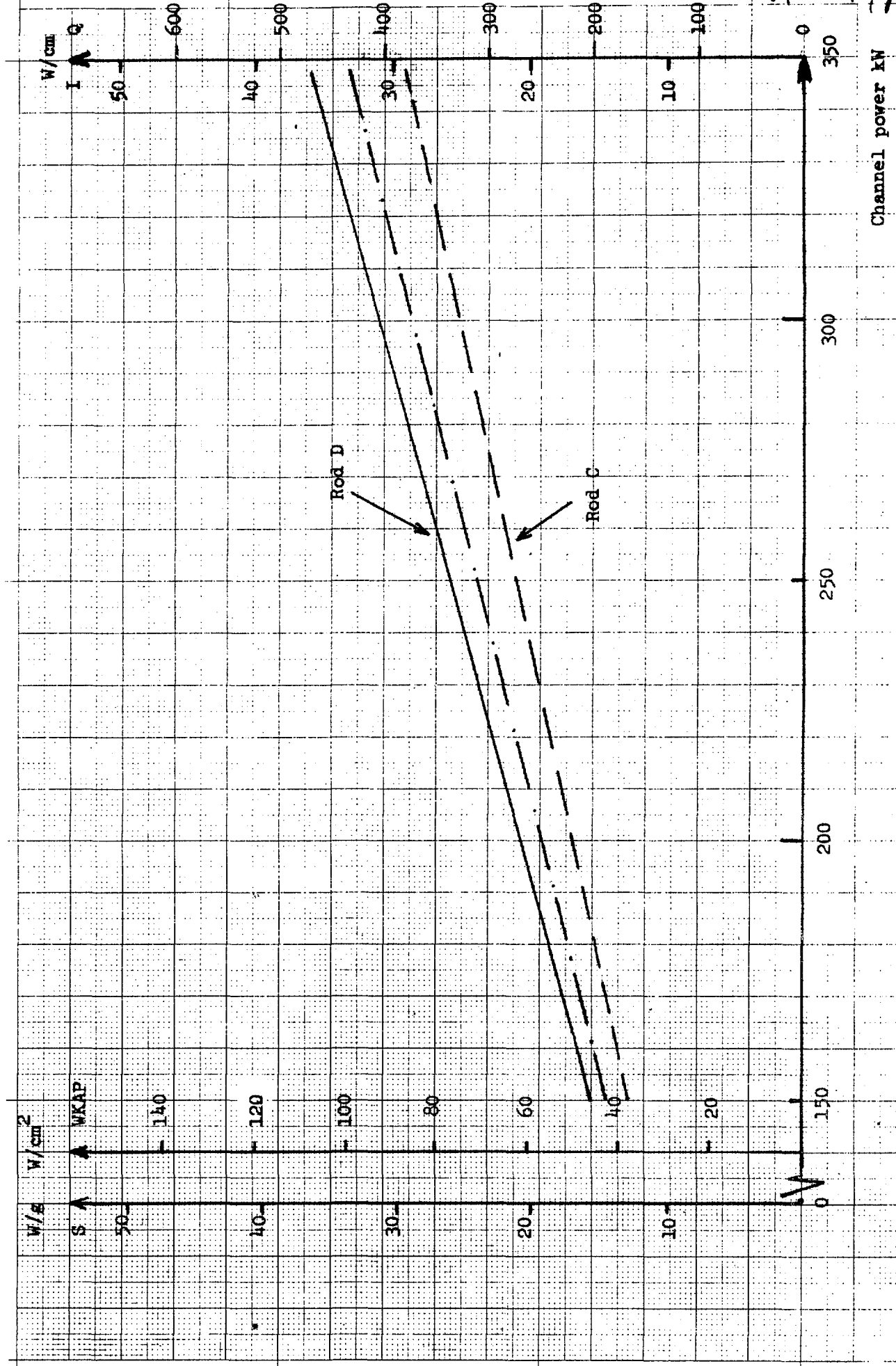
Fig. 16



Linear heat output (Q), heat conductivity integral (I), heat surface flux on the canning (WKAP) and specific power (S) as a function of channel power in axial maximum position

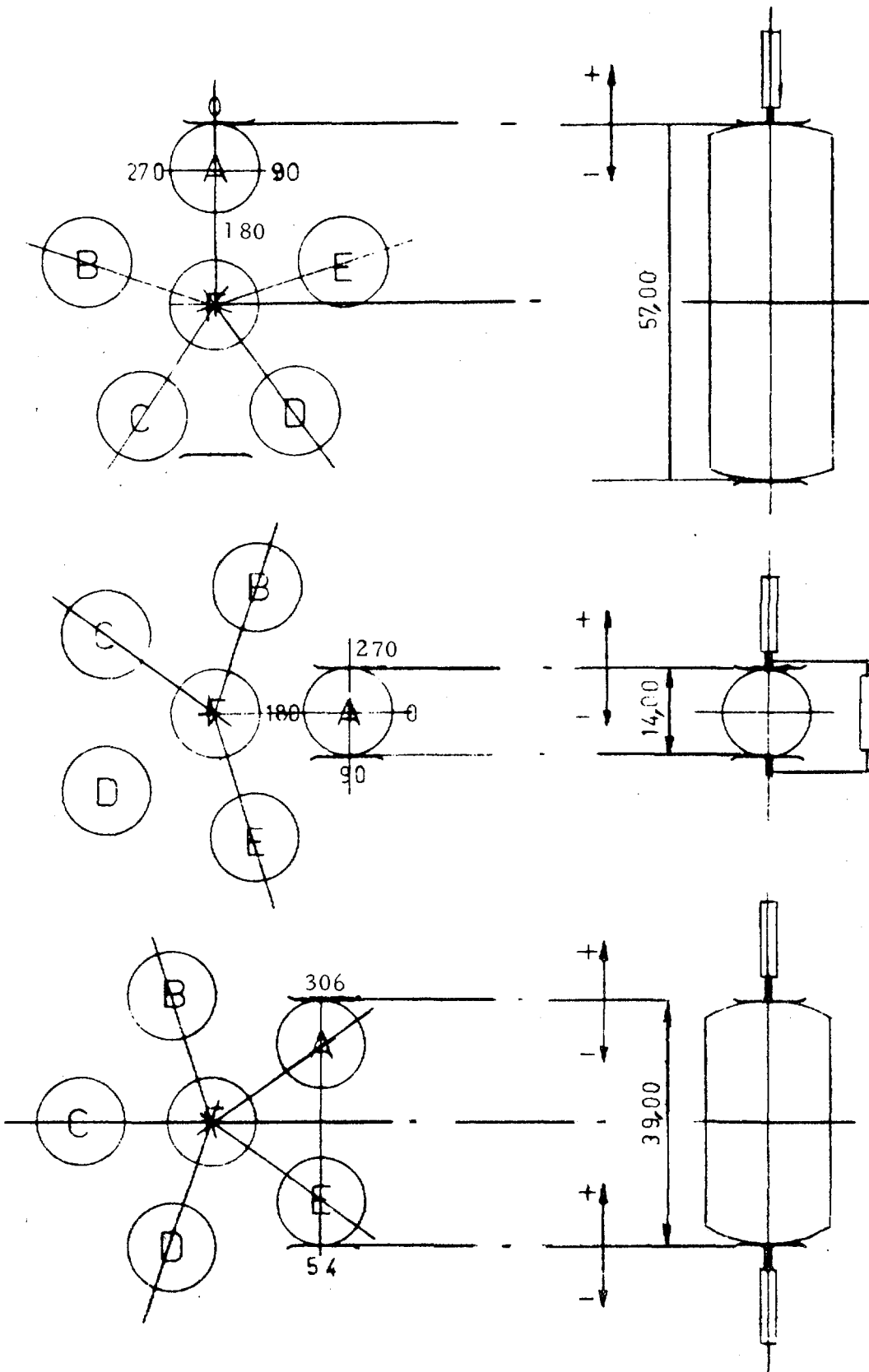
Fig. 17

67 05 29 / 97



Goliath gauges

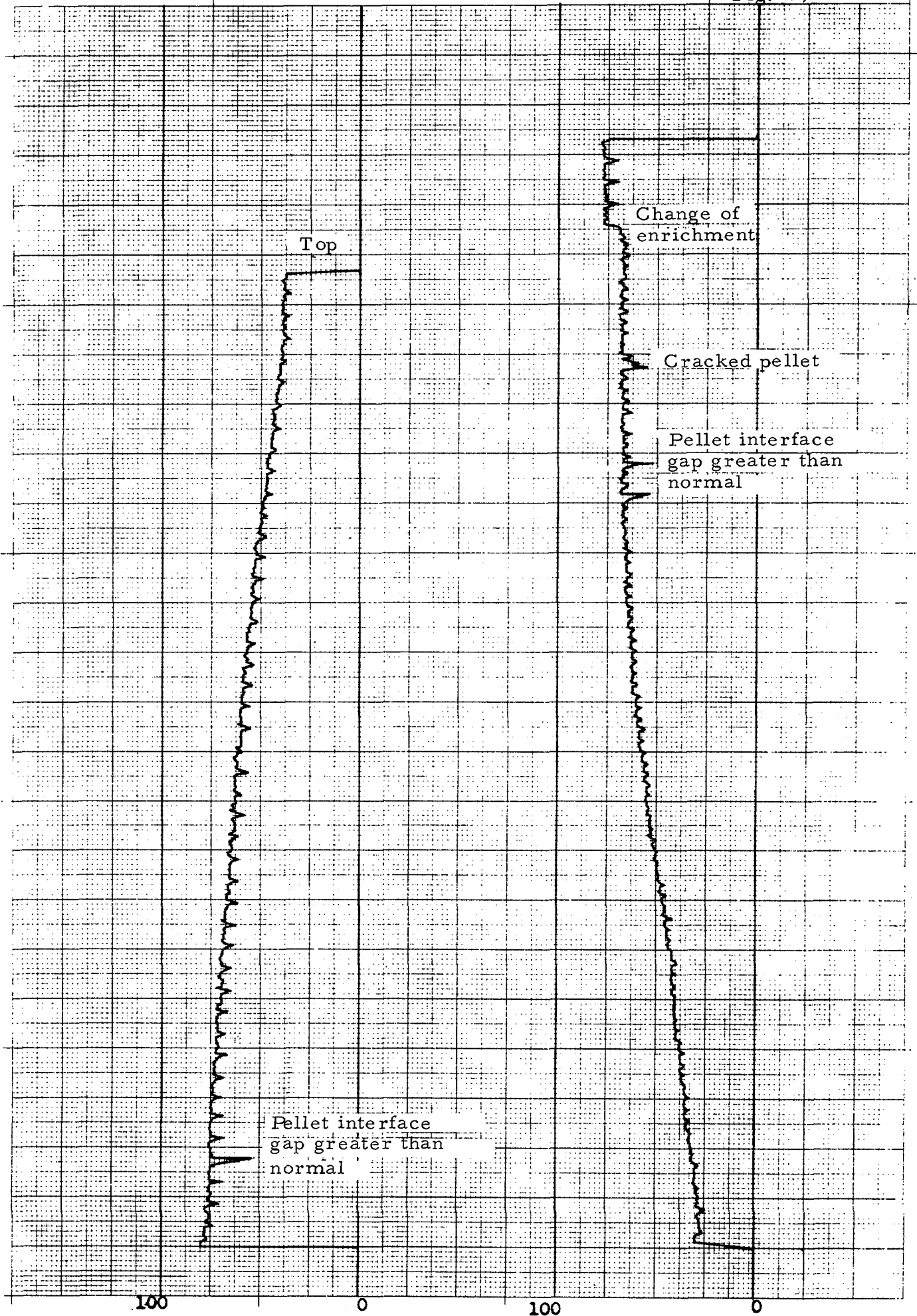
Fig. 18



Gamma-scanning

Rod A

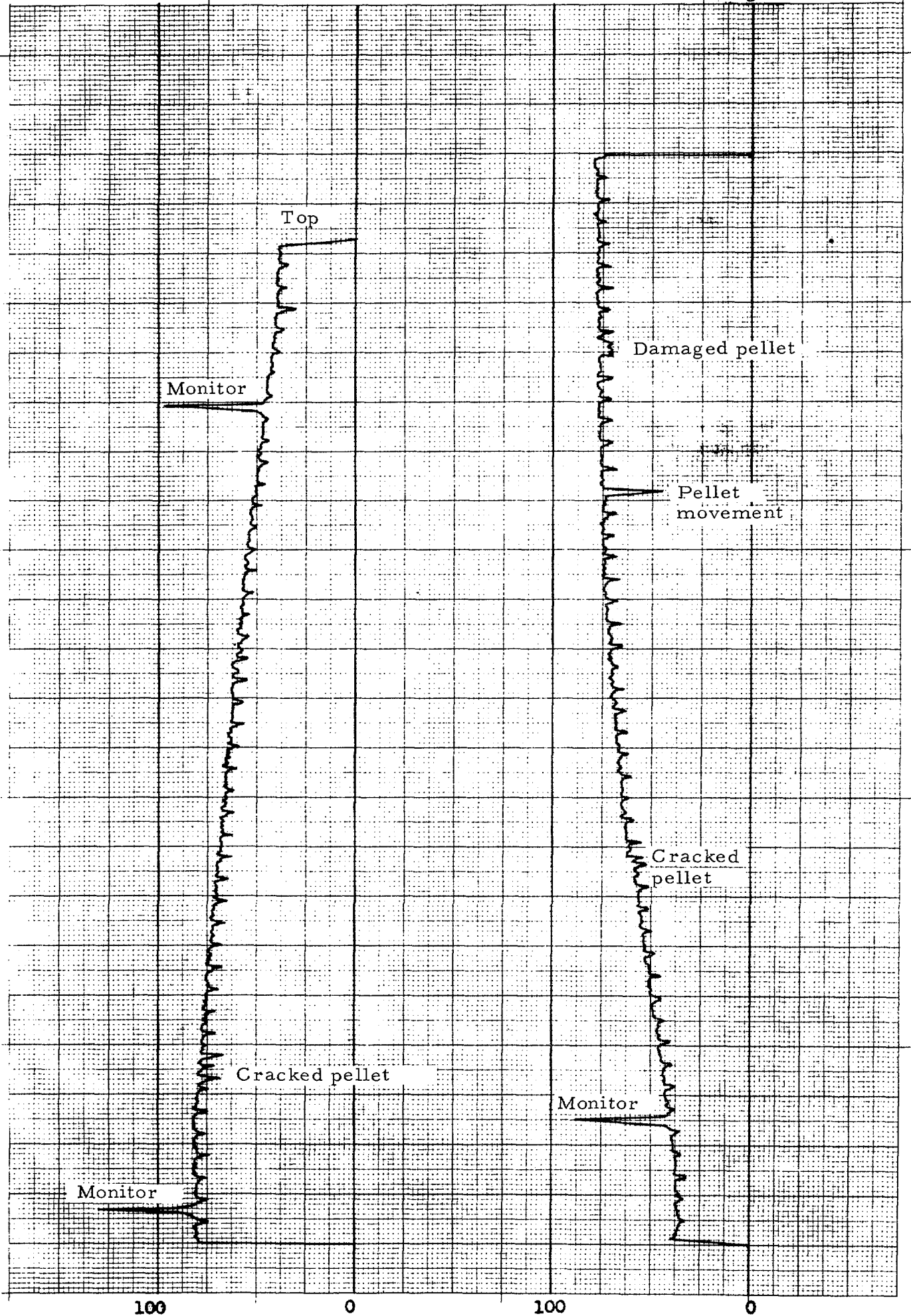
Fig. 19



Gamma-scanning

Rod B

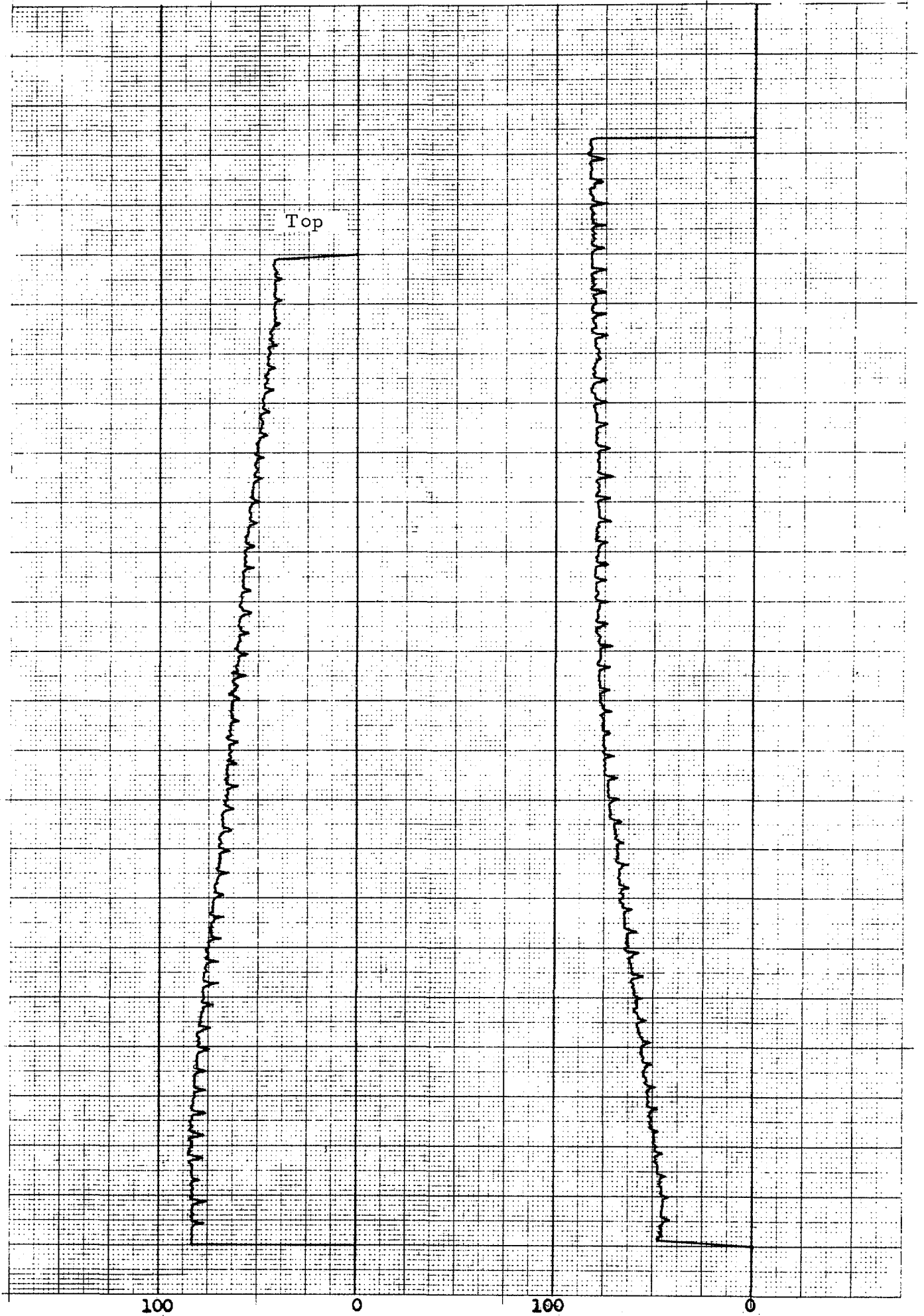
Fig. 20



Gamma-scanning

Rod C

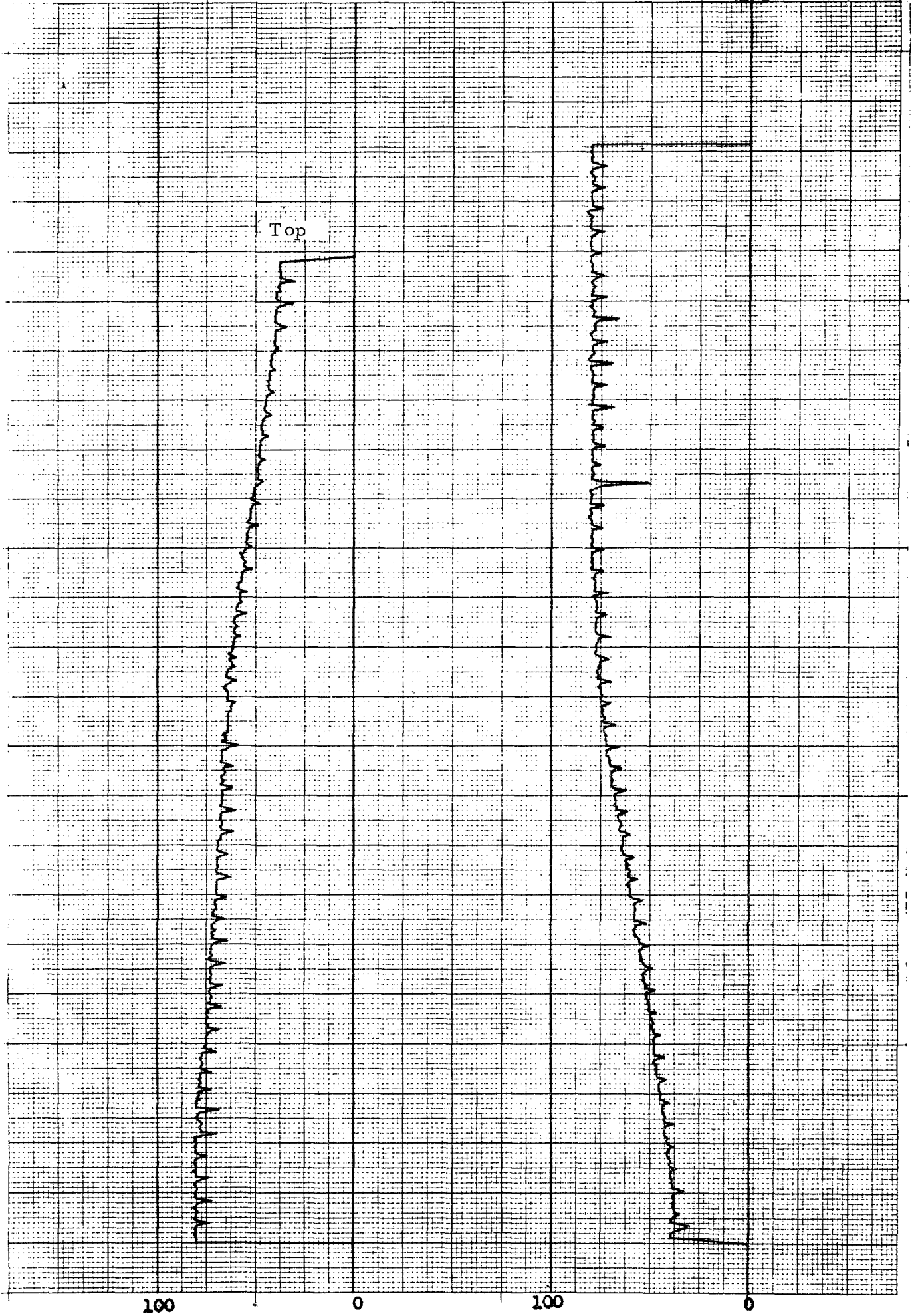
Fig. 21



Gamma-scanning

Rod D

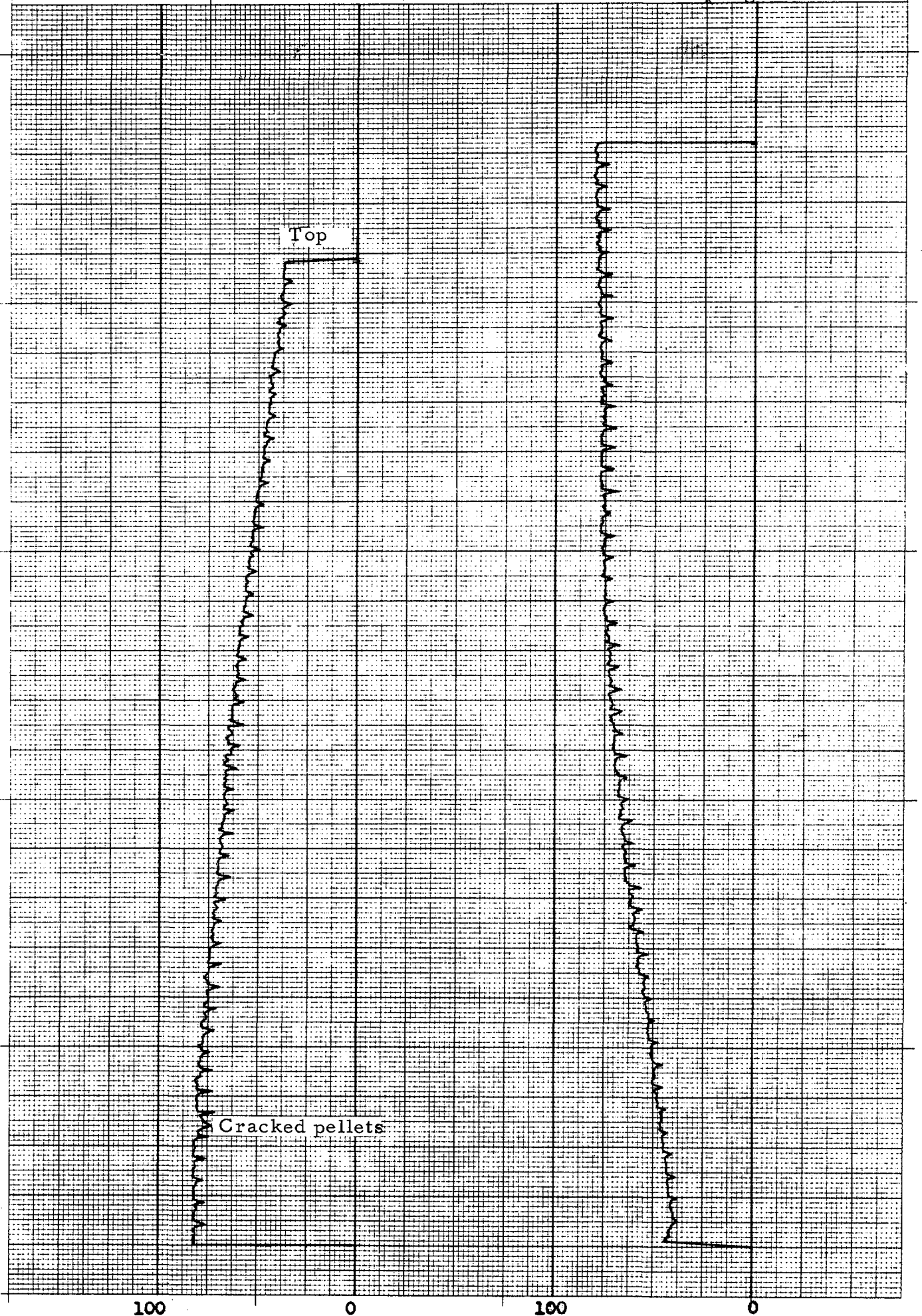
Fig. 22



Gamma-scanning

Rod E

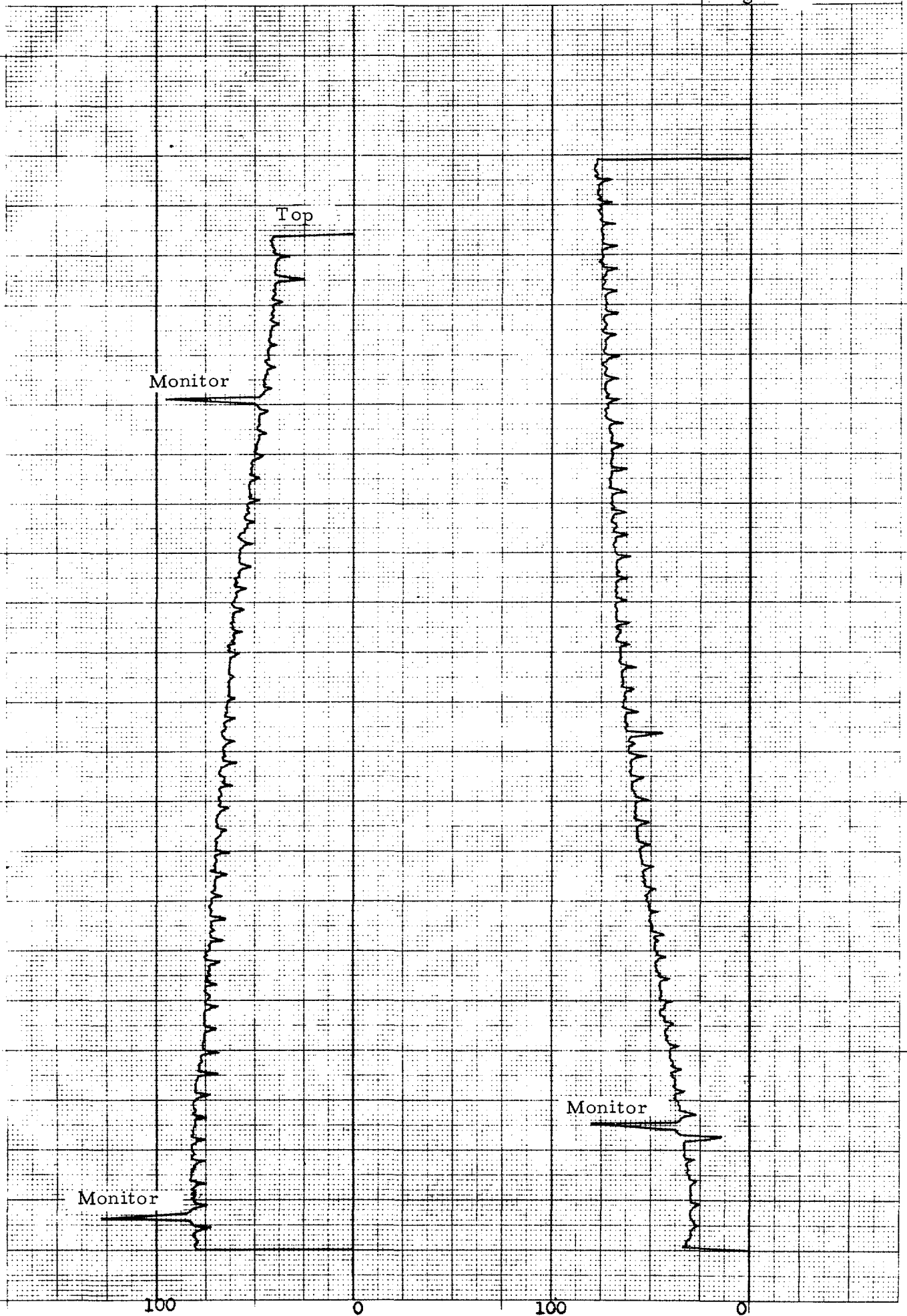
Fig. 23



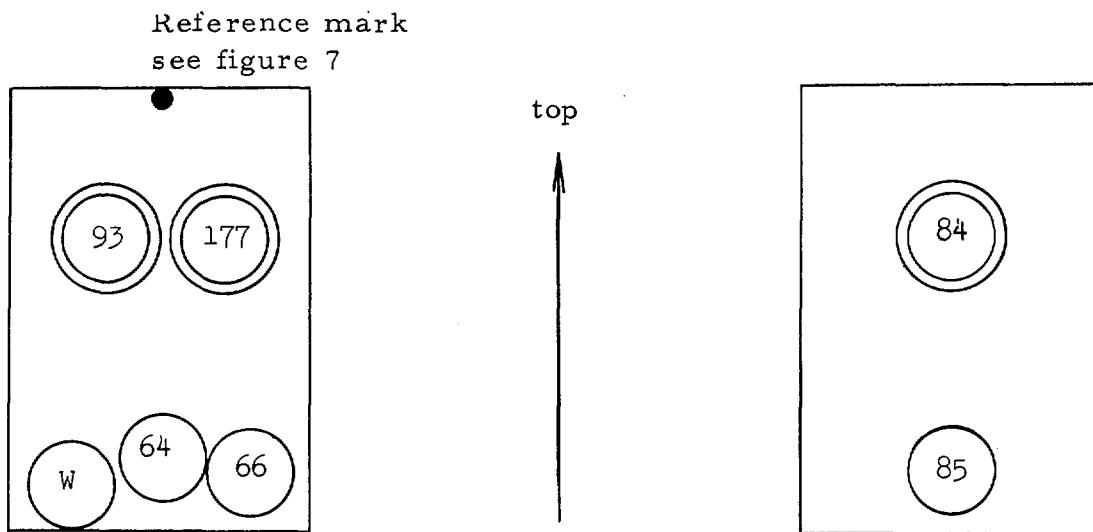
Gamma-scanning

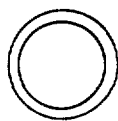
Rod F

Fig. 24



The samples for the hydride measurement



 = from spacer contact point

 = ordinary canning

W = waste

The figures in the symbols correspond to the hydride content in ppm.

